IVYSPRING INTERNATIONAL PUBLISHER

International Journal of Biological Sciences

2024; 20(10): 4044-4054. doi: 10.7150/ijbs.97434

Research Paper

Nephron-Specific *Lin28A* Overexpression Triggers Severe Inflammatory Response and Kidney Damage

Anna Futorian[1], Leah Armon[1], Hiba Waldman Ben-Asher[1], Irit Shoval[1], Inbal Hazut[2], Ariel Munitz[2], Achia Urbach[1]✉

1. The Mina and Everard Goodman Faculty of Life Sciences, Bar-Ilan University, Ramat Gan, Israel.
2. Department of Clinical Microbiology & Immunology, Faculty of Medical and Health Sciences, Tel Aviv University, Tel Aviv, Israel.

✉ Corresponding author: Achia.Urbach@biu.ac.il.

© The author(s). This is an open access article distributed under the terms of the Creative Commons Attribution License (https://creativecommons.org/licenses/by/4.0/). See http://ivyspring.com/terms for full terms and conditions.

Received: 2024.04.17; Accepted: 2024.07.07; Published: 2024.07.22

Abstract

The RNA-binding proteins LIN28A and LIN28B contribute to a variety of developmental biological processes. Dysregulation of *Lin28A* and *Lin28B* expression is associated with numerous types of tumors. This study demonstrates that *Lin28A* overexpression in the mouse nephrons leads to severe inflammation and kidney damage rather than to tumorigenesis. Notably, *Lin28A* overexpression causes inflammation only when expressed in nephrons, but not in the stromal cells of the kidneys, highlighting its cell context-dependent nature. The nephron-specific *Lin28A*-induced inflammatory response differs from previously described *Lin28B*-mediated inflammatory feedback loops as it is IL-6 independent. Instead, it is associated with the rapid upregulation of cytokines like *Cxcl1* and *Ccl2*. These findings suggest that the pathophysiological effects of *Lin28A* overexpression extend beyond cell transformation. Our transgenic mouse model offers a valuable tool for advancing our understanding of the pathophysiology of acute kidney injury, where inflammation is a key factor.

Introduction

Lin28, initially identified as a heterochronic gene in Caenorhabditis elegans, is an RNA-binding protein(1,2) that regulates gene expression through two distinct mechanisms: one blocks maturation of the *Let-7* microRNA (miRNA) family(3–6), preventing gene translation suppression by these miRNA(6–8); the other, mediated via a *Let-7*-independent pathway, directly binds to mRNAs and modifies gene expression(8–10).

In mammals, there are two paralogs, *Lin28A* and *Lin28B,* which are expressed mainly in pluripotent and multipotent stem cells. *Lin28A* and *Lin28B (*henceforth, *Lin28A/B)* play a role in various biological processes, including development, growth, metabolism, tissue regeneration, and others(7,8,11–18), via the regulation of diverse molecular pathways (for review, see(7,8,12)). For example, *Lin28A/B* regulate the activity of the mTOR pathway to promote the proliferation of neuronal progenitor cells(19), and to regulate glucose metabolism(13). Normally, *Lin28A/B* undergo downregulation upon cell differentiation and their ectopic/overexpression is associated with numerous types of pediatric and adult tumors(7,8,12,20–24).

Despite the high similarity between these paralogous genes and their common function in blocking *Let-7* maturation, these proteins differ in their cellular localization, mechanisms of *Let-7* inhibition, regulatory signals governing their expression, and spatial distribution (for reviews, see(8,12,25)). A significant piece of evidence supporting the distinct roles and functions of these two paralogous proteins is the pronounced difference in phenotypes observed among *Lin28A* knockout (KO) mice, *Lin28B* KO mice, and *Lin28A/B* double KO mice(26). Additionally, some roles have been demonstrated only for one of the two paralogs. For example, it has been shown that *Lin28A* interacts with

signaling factors of the FGF/WNT, SHH, and BMP pathways to control the elongation of the caudal body axis(15), and that *Lin28B* regulates mTOR pathway activity to enable the generation of cochlear hair cells(27). *Lin28B* overexpression (OE) was also shown to play a role in a positive feedback loop connecting inflammatory response and hematopoietic cancer formation via the NF-κB-LIN28B-IL-6-STAT3 pathway(28).

Both *Lin28A* and *Lin28B* are expressed during mouse embryonic kidney development in the nephron progenitor cap-mesenchyme (CM) cells until E13.5 and E16.5, respectively(16,17). We and others found that *Lin28A/B* regulate the balance between CM proliferation and differentiation and are required for normal nephrogenesis(16,17). Specifically, we showed that *Lin28A/B* OE during embryonic nephrogenesis in the entire kidney led to abnormal CM proliferation and development of a kidney tumor highly resembling Wilms tumor(16). Interestingly, however, specific *Lin28A/B* OE in the CM cells did not result in abnormal CM proliferation but led to the development of severe postnatal kidney damage(16). This effect was not due to abnormal embryonic kidney development, as *Lin28A/B* OE in adult nephrons produced a similar phenotype(16).

In the current study, we studied this pronounced effect of *Lin28A/B* OE on the adult kidney, focusing on *Lin28A*. Remarkably, we found that the severe kidney damage resulted from an inflammatory response induced by the overexpression of *Lin28A*. We further found that the *Lin28A*-induced inflammatory response is associated with abnormal activation of the AKT pathway. These findings extend our understanding of *Lin28A* OE impact, showing that under a specific cellular context, *Lin28* OE leads to an inflammatory response rather than tumorigenesis.

Materials and Methods

Mice

All procedures were approved by the University of Bar-Ilan Institutional Animal Care and Use Committee. The generation and maintenance of TRE-Lin28A mice were previously described (11,13,14,16). These mice were crossed with Rosa26-Lox-stop-Lox mice, as described in (11,13,14,16), to obtain homozygous TRE-*Lin28A*;Lox-stop-Lox-TetOn-rtTA. Homozygous TRE-*Lin28A*;Lox-stop-Lox-TetOn-rtTA were crossed with Six2Cre mice (Jackson Laboratories Stock #009606) or FoxD1Cre mice (Jackson Laboratories Stock #012463) to achieve nephron and stromal (respectively) cell-specific *Lin28A* OE upon Dox treatment. Doxycycline – Doxycycline (Sigma-Aldrich; 1g/L) was administered to the drinking water for different time durations, as described in the Results section. Rapamycin – Rapamycin (LC Laboratories; 4 mg/kg mouse weight) was injected intraperitoneally thrice weekly for three weeks (starting at P28). Dexamethasone – Dexamethasone (Sigma-Aldrich; 25µg) was injected intraperitoneally three times a week for a three-week period. In addition, 20 mg/L of Dexamethasone was supplemented in the drinking water.

Histology and Immunofluorescence staining: Samples were fixed with 4% paraformaldehyde diluted in PBS, dehydrated in 75% EtOH, and embedded in paraffin. Sections were cut 7-µm thick and dried overnight at 37°C. The slides were dewaxed with xylene and rehydrated through a series of washes with decreasing percentages of ethanol. Antigen retrieval was performed in 10 mM sodium citrate buffer (pH 6.0) by placing it in a pressure cooker for 15 min at a high temperature. Sections were blocked in 10% serum and incubated overnight at 4°C with the primary antibodies. Tissue sections were washed with PBS and incubated for 1 h at room temperature with secondary antibodies. Sections were treated with DAPI before mounting with mounting solution (Fluoromount-G, Thermo Fisher Scientific). For the list of antibodies, see **Table S1**.

For hematoxylin and eosin (H&E) staining, sections were paraffin-embedded. Next, the sections were stained with Harris hematoxylin solution (Kaltek) for 1 min and with eosin (Millipore) for 15 s. Mounting was conducted with DPX Mountant (Millipore).

RNA extraction and qRT-PCR analysis: Total RNA was extracted using TRI Reagent (RiboEx, GeneALL). cDNA was synthesized using iScript cDNA Synthesis kit (Bio-Rad). qRT-PCR analysis was performed using PerfecTa SYBR Green FastMix (Quantabio). β-actin was used for normalization. Relative expression was analyzed using the $2^{-\Delta\Delta Ct}$ method. The data are represented as relative expression (fold change); however, the statistical analysis was performed on the ΔΔCt values due to their linearity. For primer list, see **Table S1**.

Western Blot: Total protein was extracted from harvested kidneys. Kidneys were collected and snap-frozen in liquid nitrogen. Next, 10-20mg tissue pieces were homogenized using Bullet Blender homogenizer (Next Advance) in ice-cold lysis buffer (10 mM TrisHCl pH 7.4, 150 mM NaCl, 1 mM EDTA, 1 mM EGTA, 0.5% TritonX100, 7 M urea, protease inhibitor cocktail (Millipore), and phosphatase inhibitor cocktail (Cell Signaling)). The extracted proteins were separated by 10% acrylamide gel, followed by transfer to a nitrocellulose membrane. The membranes were blocked with 2% bovine serum

albumin in TBST (TBS with 0.05% Tween20). Then, the membranes were incubated with the appropriate antibodies and developed with EZ-ECL (Biological Industries). For the list of antibodies, see **Table S1**.

Analysis of WBC and BUN levels in the blood: WBC count was performed using the Exigo™ H400 veterinary hematology analyzer (Boule), according to the manufacturer's instructions. BUN levels were measured using the Vetscan 2 (Zoetis), according to the manufacturer's instructions.

Flow Cytometry: The kidneys were obtained from lin28A OE and littermate control mice and mashed through a 100µm strainer (431752, Corning). Cell suspensions were collected and incubated for 10 minutes with RBC lysis buffer. Staining was performed on ice after incubation with anti-CD16/ CD32 (14-0161-82, eBioscience) to reduce non-specific binding to Fc receptors. Flow cytometric analysis was performed using Gallios (Beckman-Coulter). To obtain absolute cell counts, Flow-Count Fluorosphers (#7547053, Beckman-Coulter) were used according to the manufacturer's instructions. Data were analyzed using Kaluza analysis software (Beckman-Coulter). For the list of the fluorochrome-labeled anti-mouse antibodies used, see **Table S1.**

ELISA: Protein levels of TNF-α, IL-6 and CCL2 were determined using commercially available kits (TNF-α: DY410, R&D; CCL2: DY479, R&D; and IL-6: 900-T50, Peprotech), according to the manufacturer's instructions.

RNA seq: RNA quality control – For QC of purified RNA, absorbance ratios A260:A280 and A260:A230 were assessed with NanoDrop 2000. The integrity of RNA was evaluated based on RIN acquired via capillary gel electrophoresis performed using Agilent 4200 TapeStation in combination with Agilent RNA ScreenTape System (Agilent Technologies). All RNA samples went through Dnase Treatment Kit (Qiagen) before proceeding to the next step. PolyA selection and library preparation – For library preparation, NEBNext RNA ultra II RNA library preparation kit (NEB) was used. All RNA samples underwent PolyA selection following the manufacturer's protocols. Samples were multiplexed using suitable molecular barcodes, and resulting cDNA pools were processed according to the NextSeq System Denature and Dilute Libraries guide. (Illumina). Quantification and quality control of the libraries were done using a Qubit fluorimeter and Agilent 4200 TapeStation. Next-generation sequencing - Single-read sequencing of the libraries with a read length of 75 was performed with NextSeq 500 Sequencing System using NextSeq 500/550 High Output v2 kit (75 cycles) (20024906 Illumina). PhiX Control v3 (Illumina) was added at 1% to all pools as an internal control before the sequencing. The RNA seq data has been deposited in Gene Expression Omnibus (GEO), series accession number GSE254805.

Bioinformatics analysis: Sequenced reads were mapped to the mouse reference genome sequences (mm10) using STAR. The aligned reads were quantitated by Htseq. The normalization and differentially expressed genes test were implemented by DESeq2. For Pathways and GO terms enriched analysis, the DEG list was analyzed by GeneAnalytics (https://geneanalytics.genecards.org/).

Statistical analysis: All data were generated from at least three independent experiments. P values of less than 0.05 were considered statistically significant. All analyses were performed using the GraphPad Prism software. For additional information regarding the precise analyses used, see figure legends.

Results

Nephron-specific *Lin28A* OE leads to rapid damage in diverse types of kidney cells

We have shown previously that *Lin28A/B* OE in the nephrons causes severe kidney damage(16). To further explore this effect, we used the same TRE-*Lin28A*;Lox-stop-Lox-TetOn-rtTA transgenic mice described previously(11,14,16). Crossing this strain with *Six2*-Cre mice removes the stop cassette specifically in the CM cells and their derivates, i.e., the adult nephrons. This enables a specific *Lin28A* OE upon doxycycline (Dox) treatment, which leads to severe kidney damage (**Figure 1A**). To study if the kidney damage is specific to the nephron or if *Lin28A* OE in the nephrons affects other cell types in the kidney, we performed immunofluorescent staining with markers for proximal tubules (PT), distal tubules (DT), and collecting duct (CD). Interestingly, we found that nephron-specific *Lin28A* OE damaged not only the PT and the DT but also the CD, which is derived from the ureteric bud lineage and not from the *Six2* positive nephron progenitor cells(29) (**Figure 1B,C and Figure S1A**). This observation suggests that nephron-specific *Lin28A* OE has a broad effect on the kidneys. The increased blood urea nitrogen (BUN) levels (**Figure 1D**) further confirm the severe damage caused by *Lin28A* OE. Notably, this effect of *Lin28A* OE emerges within just one week, as evidenced by H&E (**Figure S1B**) and immunostaining (**Figure 1E**). To further characterize the kidney damage and to explore its cause, we performed bulk RNA sequencing on kidneys following one, two, and five weeks of Dox treatment. The increased levels of kidney injury markers such as *Kim1* and *Ngal* (30,31) already shown after one week of Dox treatment

(**Figure 1F**) further demonstrate the pronounced and rapid kidney damage.

Lin28A OE in the nephrons triggers an inflammatory response

Principal Component Analysis (PCA) of the RNA sequencing results indicates that while all the control kidneys form a cohesive cluster, each group of *Lin28A* OE kidneys forms a distinct cluster (**Figure S2A**). Notably, however, analysis of the differentially expressed genes (DEGs, defined based on the following criteria: Log2fold > 1 or < -1; Baseman > 10; and adjusted P-value <0.05) revealed that the top GO terms associated with the *Lin28A* OE upregulated DEGs were all related to inflammatory response in all the *Lin28A* OE groups (**Figure 2A**). This unexpected observation suggests that *Lin28A* OE in the nephrons induces an inflammatory response. To validate this finding, we performed FACS analysis for different types of immune cells (**Figure 2B**). We further conducted ELISA, which revealed upregulation of CCL2 but not of IL-6 or TNFα (**Figure 2C**). Consistent with the ELISA results, the RNA seq also showed significant upregulation of *Ccl2* (**Figure S2B**). However, contrary to the ELISA results, there was upregulation of *Tnfα* at the RNA level (**Figure S2B**).

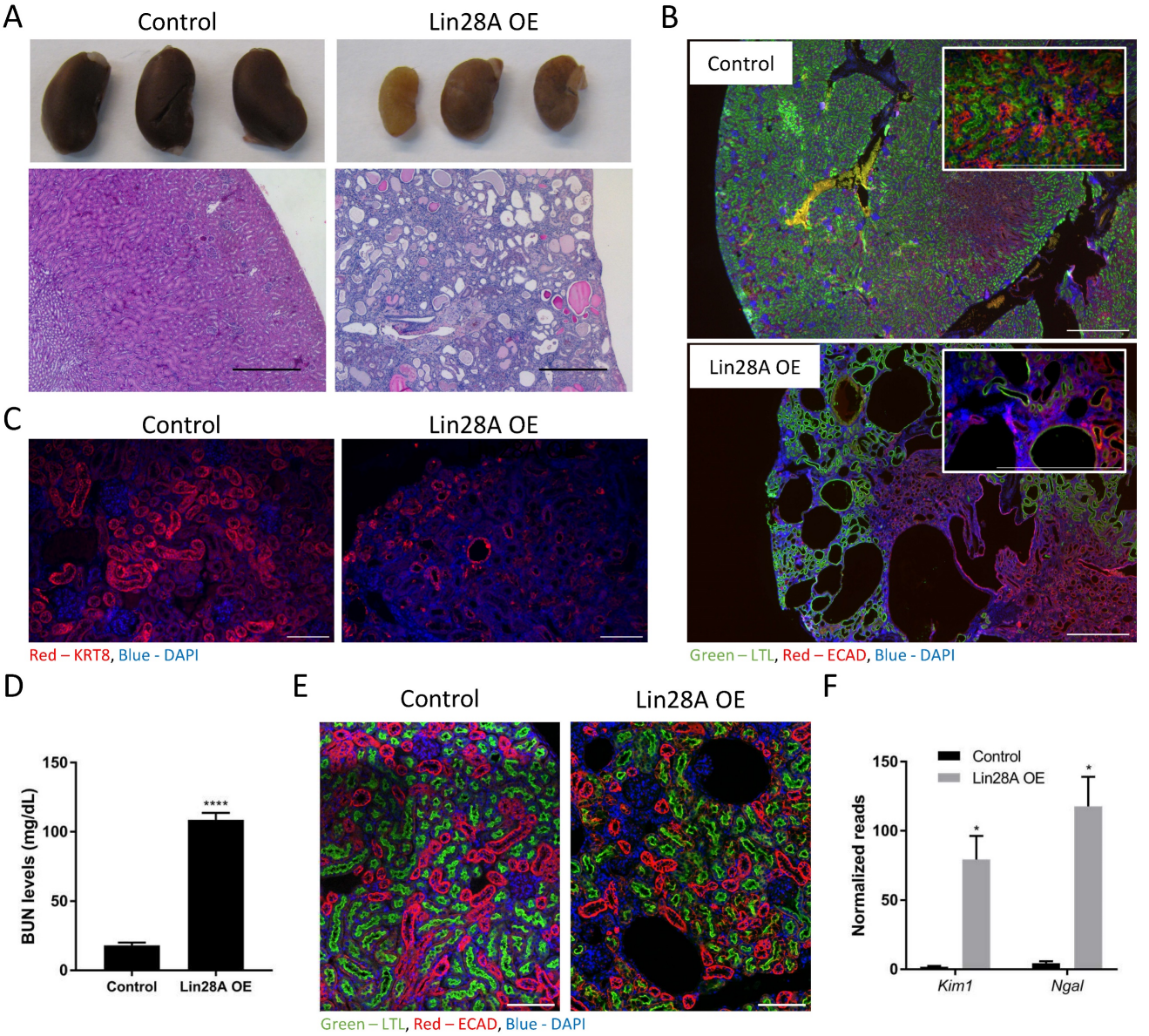

Figure 1. Nephron-specific *Lin28A* OE leads to severe kidney damage. A. Gross morphology (upper panel) and H&E staining (lower panel) of control and *Lin28A* OE kidneys following 11 weeks of *Lin28A* OE induction. Scale bar - 500μM. **B.** Control and *Lin28A* OE kidneys stained for PT (LTL) and DT/CD (ECAD) following 5 weeks of *Lin28A* OE induction. Scale bar - 500μM. **C.** Control and *Lin28A* OE kidneys stained for CD (KRT8) following 5 weeks of *Lin28A* OE induction. Scale bar - 100μM. **D.** BUN levels in control and Lin28 OE kidneys upon 3 weeks of Dox treatment. **E.** Control and Lin28 OE kidneys stained for PT (LTL) and DT/CD (ECAD) upon 1 week of Dox treatment. Scale bar - 100μM. **F.** RNA seq normalized read counts of *Kim1* and *Ngal* in *Lin28A* OE kidneys compared to control kidneys upon 1 week of Dox treatment. Statistical analysis using Student's t-test (D) or Multiple t-tests with Holm-Sidak post-test. (F). N=3. * P<0.05. **** P<0.0001.

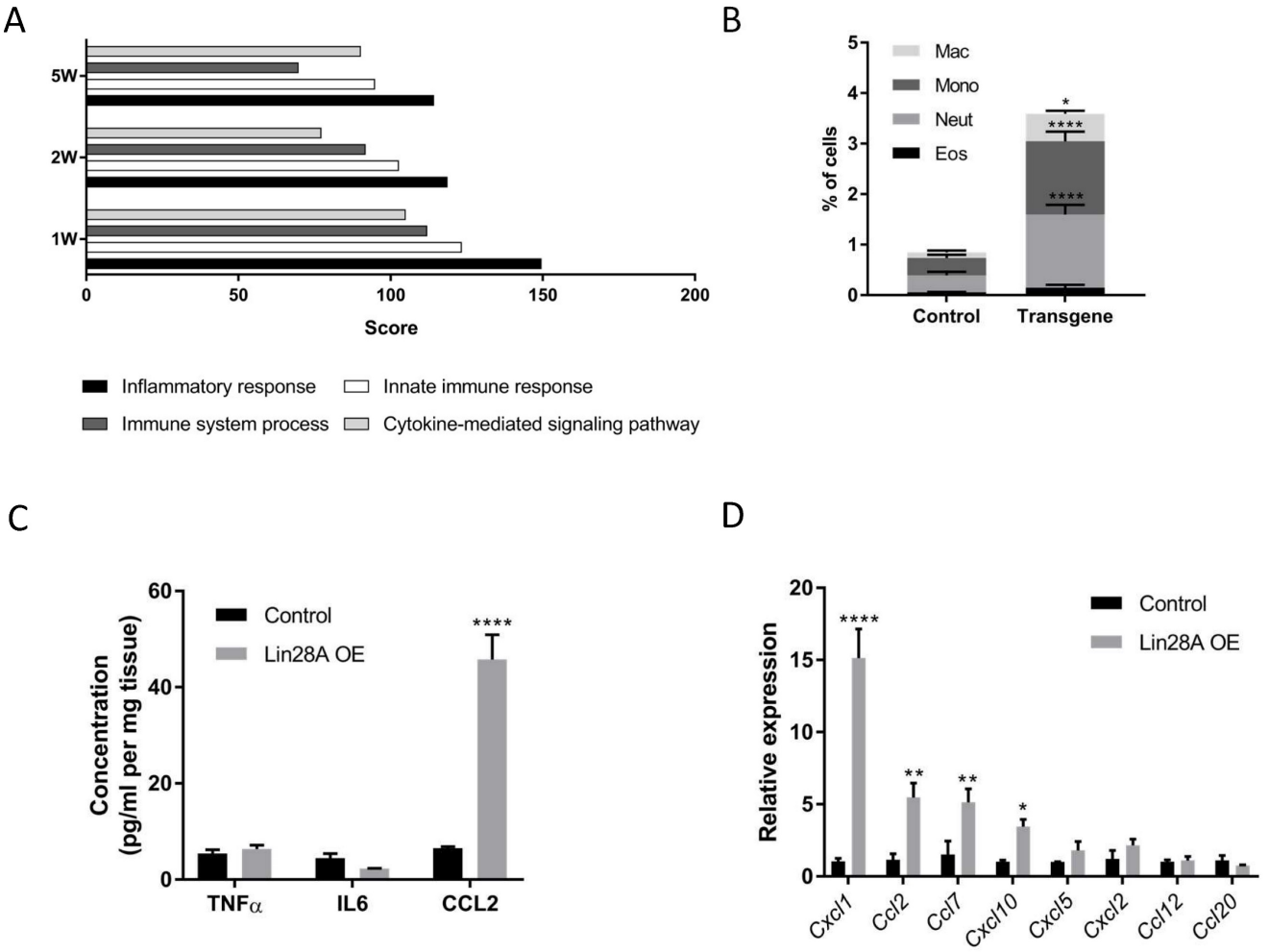

Figure 2. Nephron-specific *Lin28A* OE triggers an inflammatory response. A. Top GO terms categories of upregulated genes upon 1, 2, and 5 weeks of *Lin28A* OE. **B.** FACS analysis of immune cells in the transgenic and control kidneys. Mac – macrophages, Mono – monocytes, Neut – neutrophils, Eos – eosinophils. **C.** CCL2, IL-6, and TNFα protein levels as detected by ELISA upon 3 weeks of Dox treatment. **D.** qRT-PCR analysis for cytokines expression levels (normalized to βActin) upon 48 hours of Dox treatment. Statistical analysis using 2-way ANOVA with Sidak post-test (B, D) or multiple t-tests with Holm-Sidak post-test (C). N=3 for panels A,B,D. N=6 for panel C. * P<0.05, **P<0.01, ***P<0.001, **** P<0.0001.

We further explored if the inflammatory response was the direct effect of *Lin28A* OE or a secondary effect triggered by another kidney damage. To this end, we first generated a list of the most upregulated cytokines upon one week of Dox induction **(Table S2)**. Next, we analyzed the expression of these cytokines 48h following Dox induction (which is 24h subsequent to *Lin28A* upregulation (**Figure S2C**)). The rapid upregulation of some of these cytokines (**Figure 2D**) suggests that the inflammatory response is a direct effect of *Lin28A* OE.

As expected, DEG analysis between two weeks and one week of Dox induction showed that the trend of upregulation in genes and pathways related to the immune system was maintained between the first and the second week (**Figure S3**). Similarly, we found a trend of downregulation in genes related to metabolic pathways, indicating the worsening of kidney damage over time. Interestingly, we found only a handful of genes that changed their gene expression dynamics (from upregulation after one week to downregulation after two weeks and vice versa). It appears that this change has no functional effect, as these genes are not part of any specific pathway or GO term (**Figure S3**), and no one of them by itself is expected to play a role in the kidney phenotype (for the lists of all groups of DEGs representing gene expression dynamic, see **Table S3**).

To investigate whether the kidney damage results from the inflammatory response or if these are distinct consequences of *Lin28A* OE, we treated the mice with dexamethasone to prevent inflammation (**Figure 3A**). Remarkably, dexamethasone treatment completely rescued the kidney phenotype (**Figure 3B,C and Figure S4**). This result suggests that the *Lin28A*-induced inflammatory response caused the kidney damage. To explore whether the inflammatory response is induced when *Lin28A* is overexpressed in kidney cell types other than nephrons, we crossed the TRE-*Lin28A*;Lox-stop-Lox-TetOn-rtTA transgenic

mice with *FoxD1*-Cre mice to induce *Lin28A* OE in the stromal cells of the kidneys(32). While this crossing led to a significant *Lin28A* OE (**Figure S5A**), it did not cause an inflammatory response and kidney damage **(Figure S5A,B)**. These results indicate that the effect of *Lin28A* OE on inflammation development is cell-context-dependent.

To determine whether *Lin28A* OE is required only for the initiation of the inflammatory response or also for its maintenance, we treated the mice with Dox for 2-3 weeks and then withdrew Dox for an additional three weeks. As expected, Dox withdrawal led to *Lin28A* downregulation (**Figure S6A**). This downregulation of *Lin28A* significantly decreased the inflammatory response, as evidenced by the downregulation of CXCL1, indicating that Lin28A OE plays a role in both initiating and sustaining the inflammatory response (**Figure S6B**). Remarkably, although the decrease in the inflammatory response did not lead to recovery of the kidney phenotype, it halted further progression of the damage (**Figure S6C**).

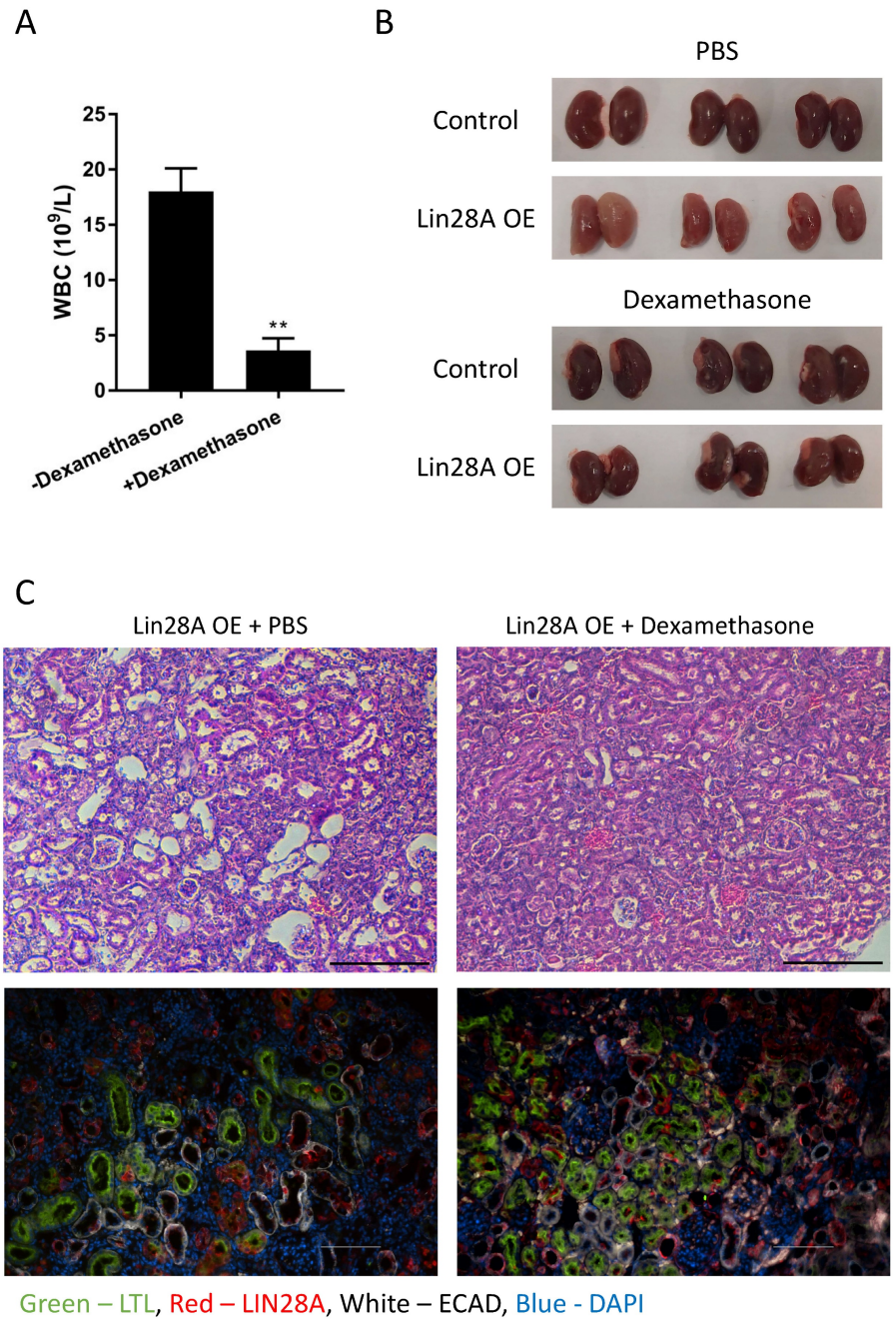

Figure 3. Dexamethasone treatment prevents *Lin28A* OE-induced kidney damage. A. White blood cell (WBC) count of *Lin28A* OE mice treated with dexamethasone/PBS for 3 weeks. **B.** Gross morphology of kidneys from *Lin28A* OE and control mice treated with dexamethasone/PBS for 3 weeks. **C.** H&E staining (upper panel) and immunostaining (lower panel) of *Lin28A* OE kidneys treated with PBS or with dexamethasone for 3 weeks. Kidneys were stained for LIN28A, PT (LTL), and DT/CD (ECAD). Scale bar - 100μM. Statistical analysis using Student's t-test. N=3. ** P<0.01.

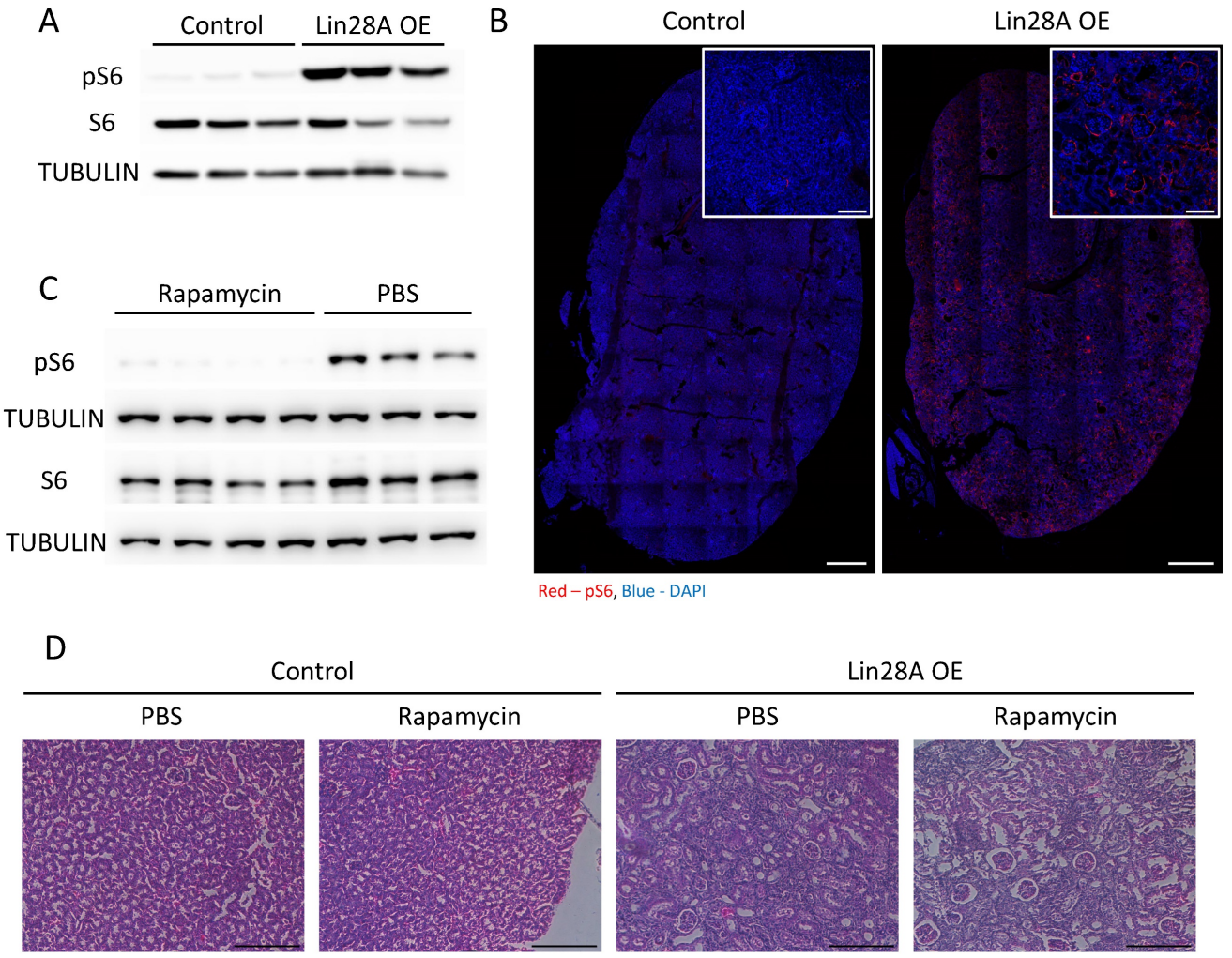

Figure 4. *Lin28A* OE leads to the activation of the mTOR pathway. A. Western blot for phospho-S6 (pS6), S6, and αTUBULIN levels in control and *Lin28A* OE kidneys (3 weeks of doxycycline treatment). **B.** pS6 immunostaining in control and *Lin28A* OE kidneys. Scale bar - 500μM, inset scale bar - 100μM. **C.** Western blot for pS6, S6, and αTUBULIN levels in *Lin28A* OE kidneys upon rapamycin or PBS treatment. **D.** H&E staining of *Lin28A* OE kidneys upon rapamycin or PBS treatment. Scale bar - 100μM.

The mTOR signaling pathway is upregulated but not involved in the kidney phenotype

It has been shown previously that *Lin28A/B* regulate the activation of the mTOR pathway(11–13), which, among other functions, regulates the immune system response(33) and whose abnormal activation has also been associated with kidney pathogenesis(34). Indeed, we observed a significant activation of the mTOR pathway (as evidenced by increased pS6 levels) upon *Lin28A* OE in the kidneys (**Figure 4A,B**). Therefore, we treated the transgenic and control mice with rapamycin to explore if the mTOR pathway is also involved in the kidney phenotype induced by *Lin28A* OE. While the rapamycin treatment significantly inhibited the activation of mTOR pathway (**Figure 4C**), it did not rescue the kidney phenotype (**Figure 4D**). These results indicate that the effect of *Lin28A* OE on the kidneys is not mediated via mTOR pathway activation.

The effect of *Lin28A* OE on the kidneys is mediated via the AKT-NF-κB-CXCL1 pathway

Our qRT-PCR and RNA seq data (**Figure 2D** and **Table S2**) reveal that *Cxcl1* is one of the most significantly upregulated cytokines upon *Lin28A* OE. We further validated this observation by analyzing the expression levels of *Cxcl1* in comparison to *Ccl2* at 24,48,96, and 168h following Dox treatment (**Figure 5A**). *Cxcl1* plays an important role in kidney inflammation and damage(35,36) and is regulated by the NF-κB pathway(37). Our RNA-seq results showed that the NF-κB pathway was one of the most significantly upregulated pathways in the transgenic kidneys (**Figure 5B**). NF-κB activation is controlled by the AKT pathway(38), which has been shown to be upregulated upon *Lin28A* and *Lin28B* overexpression (13,39). Indeed, we found that the AKT pathway was also upregulated in the *Lin28A* OE kidneys (**Figure 5B,C**). This upregulation takes place already about

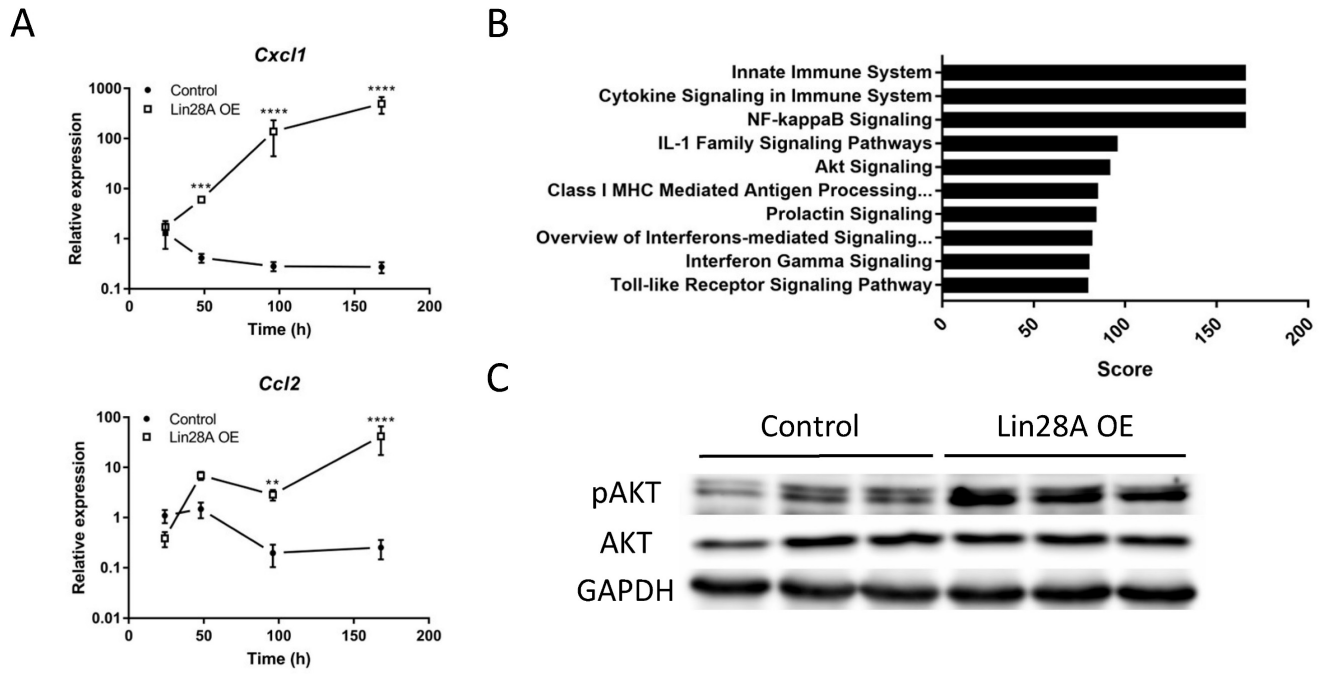

Figure 5. *Lin28A* OE-induced inflammatory response is mediated via the CXCL1-AKT-NF-κB pathway. A. Time course analysis of *Lin28A* OE induced Cxcl1 and Ccl2 expression as determined by qRT-PCR. **B.** Top 10 enriched molecular pathways in *Lin28A* OE compared to control kidneys. **C.** Western blot for phospho-AKT (pAKT), AKT, and GAPDH levels in control and *Lin28A* OE kidneys following 48h of Dox treatment. Statistical analysis using 2-way ANOVA with Sidak post-test. N=3. **P<0.01, ***P<0.001, **** P<0.0001.

24h following *Lin28A* OE (48h of Dox induction) (**Figure 5C**), indicating that this signaling pathway is a direct target of *Lin28A* OE in the transgenic kidneys. Together, these results suggest that the inflammatory response in the transgenic kidneys is mediated via the LIN28-AKT-NF-κB-CXCL1 pathway.

Discussion

Lin28A/B are primarily expressed in stem and progenitor cells, play a crucial role in diverse cellular processes (7,8,11–18) and are overexpressed in various cancer types, acting as oncogenes (for reviews, see (5,22,24,40,41)). In the current study, we show, for the first time, that *Lin28A* OE in mature nephrons results in a severe inflammatory response rather than in cell transformation. While we focused on *Lin28A*, our preliminary results ((16) and data not shown) suggest that *Lin28B* OE in the nephron may have a similar effect on the kidney.

Whereas previous studies (28,42) have focused on the oncogenic implications of *Lin28B*-mediated inflammation in hematopoietic cancers, our research emphasizes the broader impact of *Lin28A (*and probably also *Lin28B)* dysregulation on inflammatory processes. We demonstrated that *Lin28A* OE in non-hematopoietic lineage can trigger an inflammatory response via the rapid upregulation of several cytokines, including CXCL1 and CCL2, leading to severe kidney damage. This response was not associated with tumor development and was mediated via IL-6-independent mechanism. It is worth noting that the mTOR pathway, which was upregulated in the kidneys of *Lin28A* OE mice, is known to play a role in tumorigenesis (43,44). This suggests that long-term activation of this pathway via Lin28A OE, while the inflammatory response is repressed (for example, by dexamethasone treatment), might eventually result in tumor formation.

In addition to our findings, several studies have demonstrated that the lipopolysaccharide (LPS)-induced inflammatory response is mediated, in some cases, through the upregulation of *Lin28A* (45–47). Although, in contrast to our results, the involvement of *Lin28A* upregulation in the inflammatory response was LPS-dependent and was not mediated via the Lin28A-AKT-NF-κB-CXCL1 pathway, these findings further illustrate the connection between *Lin28A* upregulation and inflammation.

Additionally, a recent study investigated the impact of high glucose treatment on human mesangial cells as a model to examine the influence of elevated glucose levels on the development of diabetic nephropathy (48). In this study, the authors found a possible link between *Lin28B* upregulation and secretion of IL-6 and TNFα. This *in-vitro* model is fundamentally different from our *Lin28A* OE *in-vivo* model. The differences include the specific *Lin28* isoform, the type of cells studied, and the cytokines secreted due to *Lin28A/B* expression. Yet, their

findings provide another indication of Lin28's involvement in kidney inflammation.

To conclude, we show for the first time that *in-vivo Lin28A* OE in the nephrons can lead to a severe inflammatory response, likely via the Lin28A-AKT-NF-κB-CXCL1 pathway, independent of LPS or any other treatment. Our observation that *Lin28A* OE led to inflammation development only when overexpressed in the nephrons but not in the stromal cells of the kidney revealed that the effect of *Lin28A* OE is cell-context-dependent. However, the exact cellular conditions that lead to inflammation development due to *Lin28A* OE have yet to be determined.

One of the earliest cellular responses to acute kidney injury (AKI), which takes place within several hours of kidney damage, is neutrophil and macrophage infiltration(49–51). This initial inflammatory response can then lead to necrosis of additional renal cells, thus enhancing the inflammation(30,52,53). Therefore, we cannot rule out the possibility that the inflammatory response may be triggered by cellular damage induced by *Lin28A* OE, resulting in the secretion of damage-associated molecular patterns (DAMPs) (54). In this scenario, the AKT signaling pathway and its downstream effects might take place in immune cells recruited by the secreted DAMPs rather than in the nephron cells directly. However, we found that dexamethasone treatment not only prevented inflammation but also completely rescued the kidney phenotype. This finding along with the rapid activation of the AKT signaling pathway and the subsequent upregulation of *Cxcl1* and *Ccl2* levels within 24 hours following *Lin28A* upregulation strongly suggest that the inflammatory response is a direct effect of *Lin28A* OE.

Approximately 13.3 million patients per year are diagnosed with AKI (53,55). In addition to its acute effect, maladaptive repair of the initial kidney damage can lead to the transition of AKI to chronic kidney disorder (CKD) or worsening of baseline CKD (52,53,56). While several pathways, including inflammation, have been suggested to play a role in maladaptive AKI repair and progression of CKD, the pathophysiology of this transition is still not completely understood (52,57). Elucidating the molecular mechanisms underlying this transition will contribute to a deeper understanding of CKD pathogenesis and identify potential therapeutic targets for intervention. We demonstrated that three weeks of *Lin28A* OE followed by three weeks of its downregulation and cessation of the inflammatory response failed to recover the kidney phenotype but prevented it from becoming more severe. This observation suggests that our novel mouse model provides a valuable tool for investigating the conversion from adaptive to maladaptive repair and the development of CKD as a result of AKI. In a more general perspective, this *Lin28A* OE mouse model can be used to study other open questions regarding inflammatory kidney disorders, such as acute and chronic interstitial nephritis (58).

To summarize, our findings demonstrate that in specific cellular contexts, Lin28A OE can lead to a severe inflammatory response, resulting in significant kidney damage. These results suggest that the pathophysiological effects of Lin28A OE extend beyond cell transformation and raise the possibility that Lin28A/B OE could also play a role in human renal disorders associated with inflammatory responses.

Supplementary Material

Supplementary figures and tables.
https://www.ijbs.com/v20p4044s1.pdf

Acknowledgments

We thank Dr. Daley (Boston Children's Hospital, Boston, MA, USA) for kindly providing the Lox-stop-Lox-TetOn-*Lin28A* mice. We also thank Yael Attali-Padael and Danielle Kaim-Hagbi for their assistance with the maintenance and breeding of the mice. This project was supported in part by the Israel Science Foundation (grant #1389/15).

Author contributions

A.F. Performed the experiments and analyzed the data. L.A. analyzed the data and wrote the manuscript. H.W.B-A. performed the bioinformatics analysis**.** I.S. performed the confocal microscopy. I.H. conducted the ELISA and FACS analysis. A.M. designed and analyzed the immunological characterization. A.U. conceived and designed the study, analyzed the data, and wrote the manuscript.

Competing Interests

The authors have declared that no competing interest exists.

References

1. Ambros V, Horvitz HR. Heterochronic mutants of the nematode Caenorhabditis elegans. Science. 1984;226(4673):409–16.
2. Moss EG, Lee RC, Ambros V. The cold shock domain protein LIN-28 controls developmental timing in C. elegans and is regulated by the lin-4 RNA. Cell. 1997 Mar 7;88(5):637–46.
3. Heo I, Joo C, Kim YK, Ha M, Yoon MJ, Cho J, et al. TUT4 in Concert with Lin28 Suppresses MicroRNA Biogenesis through Pre-MicroRNA Uridylation. Cell. 2009;138(4):696–708.
4. Nam Y, Chen C, Gregory RI, Chou JJ, Sliz P. Molecular basis for interaction of let-7 MicroRNAs with Lin28. Cell. 2011;147(5):1080–91.
5. Jiang S, Baltimore D. RNA-binding protein Lin28 in cancer and immunity. Cancer Letters. 2016;375:108–13.

6. Viswanathan SR, Daley GQ, Gregory RI. Selective blockade of microRNA processing by Lin28. Science. 2008;320:97–100.
7. Viswanathan SR, Daley GQ. Lin28: A microRNA regulator with a macro role. Cell. 2010 Feb 19;140(4):445–9.
8. Shyh-Chang N, Daley GQ. Lin28: Primal regulator of growth and metabolism in stem cells. Vol. 12, Cell Stem Cell. 2013. p. 395–406.
9. Peng S, Chen LL, Lei XX, Yang L, Lin H, Carmichael GG, et al. Genome-wide studies reveal that Lin28 enhances the translation of genes important for growth and survival of human embryonic stem cells. Stem Cells. 2011;29(3):496–504.
10. Wilbert ML, Huelga SC, Kapeli K, Stark TJ, Liang TY, Chen SX, et al. LIN28 binds messenger RNAs at GGAGA motifs and regulates splicing factor abundance. Mol Cell. 2012;48(2):195–206.
11. Zhu H, Shah S, Shyh-Chang N, Shinoda G, Einhorn WS, Viswanathan SR, et al. Lin28a transgenic mice manifest size and puberty phenotypes identified in human genetic association studies. Nat Genet. 2010;42:626–30.
12. Thornton JE, Gregory RI. How does Lin28 let-7 control development and disease? Trends in Cell Biology. 2012;22(9):474–82.
13. Zhu H, Ng SC, Segr A V., Shinoda G, Shah SP, Einhorn WS, et al. The Lin28/let-7 axis regulates glucose metabolism. Cell. 2011;147(1):81–94.
14. Komarovsky Gulman N, Armon L, Shalit T, Urbach A. Heterochronic regulation of lung development via the Lin28-Let-7 pathway. FASEB J. 2019 Nov;33(11):12008–18.
15. Robinton DA, Chal J, Lummertz da Rocha E, Han A, Yermalovich A V., Oginuma M, et al. The Lin28/let-7 Pathway Regulates the Mammalian Caudal Body Axis Elongation Program. Dev Cell. 2019 Feb 11;48(3):396-405.e3.
16. Urbach A, Yermalovich A, Zhang J, Spina CS, Zhu H, Perez-Atayde AR, et al. Lin28 sustains early renal progenitors and induces Wilms tumor. Genes Dev. 2014 May 1;28(9):971–82.
17. Yermalovich A V, Osborne JK, Sousa P, Han A, Kinney MA, Chen MJ, et al. Lin28 and let-7 regulate the timing of cessation of murine nephrogenesis. Nat Commun. 2019 Jan 11;10(1):168.
18. Osborne JK, Kinney MA, Han A, Akinnola KE, Yermalovich A V, Vo LT, et al. Lin28 paralogs regulate lung branching morphogenesis. Cell Rep. 2021 Jul 20;36(3):109408.
19. Yang M, Yang SL, Herrlinger S, Liang C, Dzieciatkowska M, Hansen KC, et al. Lin28 promotes the proliferative capacity of neural progenitor cells in brain development. Development (Cambridge). 2015;142(9):1616–27.
20. Zhang J, Ratanasirintrawoot S, Chandrasekaran S, Wu Z, Ficarro SB, Yu C, et al. LIN28 Regulates Stem Cell Metabolism and Conversion to Primed Pluripotency. Cell Stem Cell. 2016 Jul 7;19(1):66–80.
21. Piskounova E, Polytarchou C, Thornton JE, LaPierre RJ, Pothoulakis C, Hagan JP, et al. Lin28A and Lin28B inhibit let-7 microRNA biogenesis by distinct mechanisms. Cell. 2011 Nov 23;147(5):1066–79.
22. Carmel-Gross I, Bollag N, Armon L, Urbach A. LIN28: A Stem Cell Factor with a Key Role in Pediatric Tumor Formation. Stem Cells Dev. 2016 Mar 1;25(5):367–77.
23. Viswanathan SR, Powers JT, Einhorn W, Hoshida Y, Ng TL, Toffanin S, et al. Lin28 promotes transformation and is associated with advanced human malignancies. Nat Genet. 2009 Jul;41(7):843–8.
24. Balzeau J, Menezes MR, Cao S, Hagan JP. The LIN28/let-7 Pathway in Cancer. Front Genet. 2017;8:31.
25. Tsialikas J, Romer-Seibert J. LIN28: roles and regulation in development and beyond. Development. 2015 Jul 15;142(14):2397–404.
26. Shinoda G, Shyh-Chang N, Yvanka De Soysa T, Zhu H, Seligson MT, Shah SP, et al. Fetal deficiency of Lin28 programs life-long aberrations in growth and glucose metabolism. Stem Cells. 2013;31:1563–73.
27. Li XJ, Doetzlhofer A. LIN28B/let-7 control the ability of neonatal murine auditory supporting cells to generate hair cells through mTOR signaling. Proc Natl Acad Sci U S A. 2020 Sep 8;117(36):22225–36.
28. Iliopoulos D, Hirsch HA, Struhl K. An epigenetic switch involving NF-kappaB, Lin28, Let-7 MicroRNA, and IL6 links inflammation to cell transformation. Cell. 2009 Nov 13;139(4):693–706.
29. Rivera MN, Haber DA. Wilms' tumour: connecting tumorigenesis and organ development in the kidney. Nat Rev Cancer. 2005;5:699–712.
30. Zuk A, Bonventre J V. Acute kidney injury. Annu Rev Med. 2016;67:293–307.
31. Vaidya VS, Ferguson MA, Bonventre J V. Biomarkers of acute kidney injury. Annu Rev Pharmacol Toxicol. 2008;48:463–93.
32. Humphreys BD, Lin SL, Kobayashi A, Hudson TE, Nowlin BT, Bonventre J V., et al. Fate tracing reveals the pericyte and not epithelial origin of myofibroblasts in kidney fibrosis. Am J Pathol. 2010;176(1):85–97.
33. Powell JD, Pollizzi KN, Heikamp EB, Horton MR. Regulation of immune responses by mTOR. Annu Rev Immunol. 2012;30:39–68.
34. Nechama M, Makayes Y, Resnick E, Meir K, Volovelsky O. Rapamycin and dexamethasone during pregnancy prevent tuberous sclerosis complex-associated cystic kidney disease. JCI Insight. 2020 Jul 9;5(13).
35. Wu CL, Yin R, Wang SN, Ying R. A Review of CXCL1 in Cardiac Fibrosis. Front Cardiovasc Med. 2021;8.
36. Hermert D, Martin I V., Reiss LK, Liu X, Breitkopf DM, Reimer KC, et al. The nucleic acid binding protein YB-1-controlled expression of CXCL-1 modulates kidney damage in liver fibrosis. Kidney Int. 2020 Apr 1;97(4):741–52.
37. Wang DT, Huang RH, Cheng X, Zhang ZH, Yang YJ, Lin X. Tanshinone IIA attenuates renal fibrosis and inflammation via altering expression of TGF-β/Smad and NF-κB signaling pathway in 5/6 nephrectomized rats. Int Immunopharmacol. 2015;26(1):4–12.
38. Ozes ON, Mayo LD, Gustin JA, Pfeffer SR, Pfeffer LM, Donner DB. NF-kappaB activation by tumour necrosis factor requires the Akt serine-threonine kinase. Nature. 1999 Sep 2;401(6748):82–5.
39. Wang XW, Li Q, Liu CM, Hall PA, Jiang JJ, Katchis CD, et al. Lin28 Signaling Supports Mammalian PNS and CNS Axon Regeneration. Cell Rep. 2018 Sep 4;24(10):2540-2552.e6.
40. Wang H, Zhao Q, Deng K, Guo X, Xia J. Lin28: an emerging important oncogene connecting several aspects of cancer. Tumour Biol. 2016 Mar 1;37(3):2841–8.
41. Nguyen LH, Zhu H. Lin28 and let-7 in cell metabolism and cancer. Transl Pediatr. 2015 Jan;4(1):4–11.
42. Beachy SH, Onozawa M, Chung YJ, Slape C, Bilke S, Francis P, et al. Enforced expression of Lin28b leads to impaired T-cell development, release of inflammatory cytokines, and peripheral T-cell lymphoma. Blood. 2012 Aug 2;120(5):1048–59.
43. Hanahan D, Weinberg RA. Hallmarks of cancer: The next generation. Vol. 144, Cell. 2011. p. 646–74.
44. Conciatori F, Ciuffreda L, Bazzichetto C, Falcone I, Pilotto S, Bria E, et al. mTOR Cross-Talk in Cancer and Potential for Combination Therapy. Cancers (Basel). 2018 Jan 19;10(1).
45. Chen IT, Cheng AC, Liu YT, Yan C, Cheng YC, Chang CF, et al. Persistent TLR4 Activation Promotes Hepatocellular Carcinoma Growth through Positive Feedback Regulation by LIN28A/Let-7g miRNA. Int J Mol Sci. 2022 Aug 1;23(15).
46. Yue Y, Zhang D, Jiang S, Li A, Guo A, Wu X, et al. LIN28 expression in rat spinal cord after injury. Neurochem Res. 2014;39(5):862–74.
47. Ni SY, Xu WT, Liao GY, Wang YL, Li J. LncRNA HOTAIR Promotes LPS-Induced Inflammation and Apoptosis of Cardiomyocytes via Lin28-Mediated PDCD4 Stability. Inflammation. 2021 Aug 1;44(4):1452–63.
48. Rong L, Xue H, Hao J, Liu J, Xu H. Long non-coding RNA MEG3 silencing weakens high glucose-induced mesangial cell injury by decreasing LIN28B expression by sponging and sequestering miR-23c. Kidney Res Clin Pract. 2023 Dec 11;
49. Swaminathan S, Griffin MD. First responders: Understanding monocyte-lineage traffic in the acutely injured kidney. Kidney Int. 2008;74(12):1509–11.
50. Li L, Huang L, Sung SSJ, Vergis AL, Rosin DL, Rose CE, et al. The chemokine receptors CCR2 and CX3CR1 mediate monocyte/macrophage trafficking in kidney ischemia-reperfusion injury. Kidney Int. 2008;74(12):1526–37.
51. Kumar S, Liu J, McMahon AP. Defining the acute kidney injury and repair transcriptome. Semin Nephrol. 2014;34(4):404–17.
52. Yu SMW, Bonventre J V. Acute kidney injury and maladaptive tubular repair leading to renal fibrosis. Curr Opin Nephrol Hypertens. 2020;29(3):310–8.

53. Zuk A, Bonventre J V. Recent advances in acute kidney injury and its consequences and impact on chronic kidney disease. Curr Opin Nephrol Hypertens. 2019;28(4):397–405.
54. Huang Y, Jiang W, Zhou R. DAMP sensing and sterile inflammation: intracellular, intercellular and inter-organ pathways. Nat Rev Immunol. 2024 Apr 29;
55. Mehta RL, Cerdá J, Burdmann EA, Tonelli M, García-García G, Jha V, et al. International Society of Nephrology's 0by25 initiative for acute kidney injury (zero preventable deaths by 2025): A human rights case for nephrology. The Lancet. 2015 Jun 27;385(9987):2616–43.
56. Chawla LS, Eggers PW, Star RA, Kimmel PL. Acute kidney injury and chronic kidney disease as interconnected syndromes. N Engl J Med. 2014 Jul 3;371(1):58–66.
57. Fu Y, Tang C, Cai J, Chen G, Zhang D, Dong Z. Rodent models of AKI-CKD transition. Am J Physiol Renal Physiol. 2018 Oct 5;315(4):F1098–106.
58. Praga M, González E. Acute interstitial nephritis. Kidney Int. 2010 Jun;77(11):956–61.